NASA TECHNICAL NOTE

NASA TN D-2715

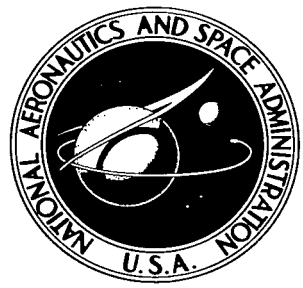

c. 1

TECH LIBRARY KAFB, NM
0079731

NASA TN D-2715

INFLUENCE OF SOLAR RADIATION PRESSURE ON ORBITAL ECCENTRICITY OF A GRAVITY-GRADIENT-ORIENTED LENTICULAR SATELLITE

by William M. Adams, Jr., and Ward F. Hodge

Langley Research Center
Langley Station, Hampton, Va.

NATIONAL AERONAUTICS AND SPACE ADMINISTRATION • WASHINGTON, D. C. • MARCH 1965

TECH LIBRARY KAFB, NM
0079731

INFLUENCE OF SOLAR RADIATION PRESSURE ON ORBITAL ECCENTRICITY OF A GRAVITY-GRADIENT-ORIENTED LENTICULAR SATELLITE

By William M. Adams, Jr., and Ward F. Hodge

Langley Research Center
Langley Station, Hampton, Va.

NATIONAL AERONAUTICS AND SPACE ADMINISTRATION

For sale by the Office of Technical Services, Department of Commerce,
Washington, D.C. 20230 -- Price $1.00

INFLUENCE OF SOLAR RADIATION PRESSURE ON ORBITAL ECCENTRICITY OF A GRAVITY-GRADIENT-ORIENTED LENTICULAR SATELLITE

By William M. Adams, Jr., and Ward F. Hodge
Langley Research Center

SUMMARY

A method is presented for calculating the perturbations of the orbital elements of a low-density lenticular satellite due to solar radiation pressure. The necessary calculations are performed by means of the digital computer. Typical results are presented for seven orbital inclinations ranging from 0° to 113° for a perfectly absorptive satellite initially in a nearly circular 2,000-nautical-mile orbit.

The information obtained indicates that the change in eccentricity caused by solar radiation pressure becomes large enough for all the inclinations considered to cause attitude-control problems with the gravity-gradient stabilization system. A nearly circular orbit appears necessary for lenticular satellites since the ability of gravity gradient attitude control systems to damp the pitching libration induced by elliptic orbital motion is still in doubt. The results also indicate that the effects of solar radiation pressure on the orbital eccentricities of lenticular and spherical satellites are nearly the same when the two configurations are compared on an equal area-mass ratio basis.

INTRODUCTION

The satellite systems currently being considered as a means of establishing worldwide communications networks include passive reflectors such as Echo-type inflatable balloon structures. It is shown in reference 1 that for this type of satellite, economic considerations make it desirable to increase the usable reflecting area per unit weight in orbit over that of the Echo sphere. Inflatable lenticular configurations offer the possibility of obtaining a communications surface equivalent to that provided by a sphere of equal radius at a sizable reduction in satellite mass. However, a lenticular satellite requires attitude control since its symmetry axis must be continuously oriented parallel to the local vertical along its orbital path in order to function properly as a passive communications link.

Damped gravity-gradient systems similar to that described in reference 2 are being considered as a passive means of providing the necessary attitude control. However, the use of such systems requires a nearly circular orbit to prevent the pitching libration of the satellite that is induced by eccentric orbital motion from causing unstable attitude motion. (See refs. 3 and 4.) For the large area-mass ratio required to achieve a significant weight reduction, the satellite is subject to strong perturbations due to solar radiation pressure. These perturbations have been widely investigated for low-density spherical satellites. (See refs. 5 to 12.) In most instances, the principal effect is a large-amplitude variation in the orbital eccentricity which can shorten satellite lifetimes appreciably and can cause difficulty in maintaining the uniform spacing between satellites that is necessary for continuous communications service. Since these problems would be expected for any satellite having a large area-mass ratio, the problem of interest here is whether solar radiation pressure will cause the orbital motion of a low-density lenticular satellite to become sufficiently eccentric to render gravity-gradient attitude stabilization ineffective.

A primary consideration in investigating this problem is the large effect the satellite's optical and physical properties can have on the vector character of the resultant force exerted on it by solar radiation pressure. These parameters can vary the direction of the resultant force relative to that of the incident force and can alter the magnitude of the resultant force from zero for an ideal transmitter to twice that of the incident force for a perfect specular reflector. Thus, the choice of materials and construction of the satellite surface can alter the nature of the problem considerably.

Although it may eventually prove possible to effectively avoid solar pressure perturbations by using mesh materials or some other means, it is currently of interest to establish how severe the problem is for a lenticular satellite having a continuous solid surface. Of these types of surfaces, the perfect absorber appears most desirable unless suitable materials that are highly transmissive are developed. No net torques are exerted on a symmetrical ideal absorber by solar radiation pressure and the magnitude of the resultant force is the minimum for any type of opaque surface. For these reasons, it was decided to assume a perfectly absorptive satellite for the study described in the present report. This approach simplifies the calculation of solar pressure perturbations considerably and permits the best comparison with the sphere.

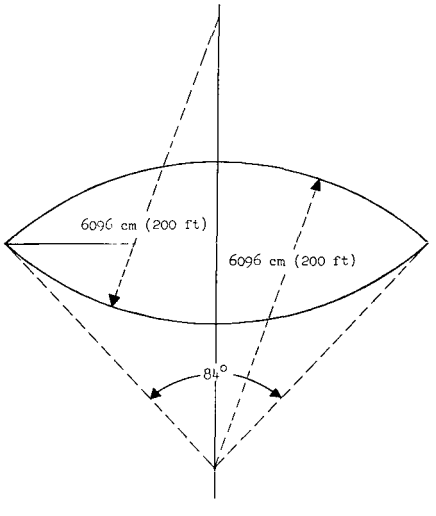

Figure 1.- Lenticular satellite configuration.

The results contained in this report were calculated for the 770-pound, 200-foot-radius lenticular satellite illustrated in figure 1. Data for seven orbital inclinations were calculated by means of numerical integration on the digital computer for a 2,000-nautical-mile circular orbit. Corresponding data for a sphere

are also presented for two of the seven cases. Since resonances which can occur for certain orientations of the orbit plane relative to the disturbing force can produce the largest changes in eccentricity, it is important to examine their effects on the orbital motion of lenticular satellites. For this reason, the seven inclinations used in the study were chosen to include some of the resonant conditions that might be encountered.

SYMBOLS

Bars appearing over symbols denote vectors the magnitudes of which are indicated by omitting the bars. In instances where more compact notation is desirable, a dot placed above a symbol is used to denote differentiation with respect to time. Symbols used for special purposes are defined where they occur in the text and are not included in the following list.

A	area, cm^2
A_2	coefficient of second harmonic in earth's gravitational potential, km^2
a	semi-major axis, cm or km
b	semi-minor axis, cm or km
E	eccentric anomaly, deg
e	eccentricity
$\overline{F}$	acceleration vector, cm/sec^2
i	orbit inclination with respect to equator, deg
$\hat{i},\hat{j},\hat{k}$	unit vectors along the X, Y, Z axes (see fig. 4)
m	mass, gm
n	mean motion, deg/day
$\hat{P},\hat{Q},\hat{R}$	unit vectors along orbit axes (see fig. 4)
p	radiation pressure, $dynes/cm^2$
r	radius, cm or km
t	time, days
$\hat{U}$	unit vector from center of earth to sun
X,Y,Z	geocentric rectangular coordinates (see fig. 4)

α angle between satellite symmetry axis and direction to sun, deg

α_o semi-central cone angle of lens, deg (see fig. 3)

ϵ obliquity, deg

θ true anomaly, deg

λ true longitude of sun on ecliptic, deg

μ product of universal gravitational constant and mass of earth, km^3/day^2

Ω right ascension of ascending node, deg

ω argument of perigee, deg

Subscript:

o reference condition

PROCEDURE

The computational method and assumptions used in calculating the radiation pressure perturbations for a perfectly absorptive lenticular satellite are presented in this section of the report. In order to perform the desired calculations, it is necessary to account for the variation of the solar disturbing force that arises because the effective area-mass ratio is not constant for lenticular satellites. A suitable mathematical expression for this variation is obtained in closed analytical form. The result is then used to modify, for application to lenticular configurations, an existing digital computer program (Lifetime 18) developed at the NASA Goddard Space Flight Center. This program calculates the radiation pressure perturbations by numerical solution of the differential equations relating the time variations of the satellite's orbital elements to the solar disturbing force.

Assumptions

In addition to assuming a perfect black body absorber of the incident radiation, the following general assumptions were made:

(1) In comparison with the direct radiation from the sun, the total force arising from all other sources of radiation is small and is considered negligible for the purposes of this report.

(2) Emission by the satellite surface is assumed to occur isotropically so that the force due to reradiation is also negligible.

(3) The satellite is considered to have constant mass and to be sufficiently rigid so that variations in the disturbing force due to deformation and effects caused by elastic flexing may be ignored.

(4) The effects of atmospheric drag may be ignored for the 2,000-nautical-mile altitude used in the study.

(5) The solar pressure forces on the attitude-control system and any associated damper and support booms are assumed to be negligible in comparison with that exerted on the main lenticular portion of the satellite.

(6) Attitude disturbances from all sources are treated as short-period terms in the disturbing function which tend to average out, and therefore would not be expected to alter appreciably the orbital motion. (See ref. 5.)

Analytical Representation of the Solar Disturbing Function

The disturbing acceleration caused by solar radiation pressure.- The force exerted on a perfectly absorptive body by solar radiation is analogous to that arising from fluid pressure. The acceleration produced by this force is

$$\overline{F} = -p \frac{A}{m} \hat{U}$$

where p is the intensity of the radiation pressure, A/m is the area-mass ratio of the accelerated body in which A is its effective area projected normal to the sun's rays, and $\hat{U}$ is a unit vector in the direction to the sun. The minus sign arises because the positive direction of $\hat{U}$ is defined oppositely to that of $\overline{F}$. Since the quantity $p \frac{A}{m}$ is the magnitude of $\overline{F}$, the preceding equation is usually written in the form

$$\overline{F} = -F\hat{U} \tag{1}$$

The intensity of the radiation pressure varies inversely with the square of the distance to the sun s and is given by

$$p = p_o\left(\frac{s_o}{s}\right)^2 \tag{2}$$

where p_o is the intensity at the mean earth-sun distance s_o and has approximately the value 4.65×10^{-5} dyne per square centimeter. (See ref. 9.) It should be noted that without suitable modification, equation (1) does not apply in cases where the satellite surface may be partly reflective, absorptive, and transmissive. In general, the resultant force will not be directed parallel to the sun's rays and its magnitude will be altered by a factor that depends on the physical and optical properties of the satellite.

The modification for lenticular configurations.- For this type of satellite, it is necessary to account for the variation in the magnitude of $\overline{F}$ that

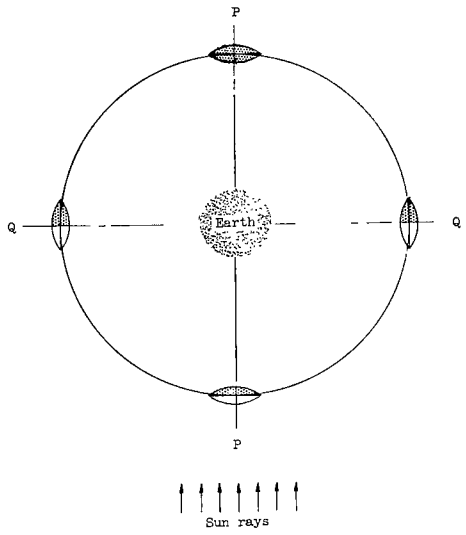

Figure 2.- Variation of effective area over a full orbital revolution.

occurs because the effective area A changes continually over each orbital revolution. The manner in which this variation occurs is illustrated in figure 2. If the sun line is parallel to the orbit plane as shown in the sketch, A will oscillate between the circular area at points P and the lenticular area at points Q with a frequency of twice the orbital period. Corresponding to this variation in area, the area-mass ratio varies from 149.66 to 50.17 cm^2/gm. It should be noted that, near one of the points P, the lenticule is in the earth's shadow at which time the effective cross-sectional area presented to the sun is zero. For the case where the sun line is normal to the orbit plane, no variation occurs and A remains equal to the lenticular area of points Q. Since the lenticule is a body of revolution, it is evident from figure 2 that, shadow effects being neglected, the variation in A is solely a function of the angle between its symmetry axis and the direction of the sun.

The approach used to obtain a suitable analytical expression for A in terms of the sun angle α is illustrated in figure 3. A lenticular body may be represented mathematically in terms of two intersecting spheres of radius r whose centers are spaced a distance 2d apart as shown on the left sketch in figure 3. With r and d specified, each half of the lenticule subtends a central angle $2\alpha_o$. For the range $0 \leqq \alpha \leqq \alpha_o$, the area A is simply that of the ellipse formed by the projection of the circular intersection of the two spheres in the direction of the sun's rays as shown on the sketch to the right in figure 3. The semi-major and semi-minor axes of this ellipse are

$$a = r \sin \alpha_o$$

and

$$b = a \cos \alpha$$

so that its equation in rectangular coordinates with the origin at its center is

$$\frac{x^2}{a^2} + \frac{y^2}{b^2} = 1 \tag{3}$$

The area of this ellipse is

$$A = \pi r^2 \sin^2 \alpha_o \cos \alpha \tag{4}$$

For the range $\alpha_o \leqq \alpha \leqq \frac{\pi}{2}$, transition to the lenticular area of points Q in figure 2 adds crescent-shaped areas to each half of the ellipse which are bound by equation (3) and the circles

$$x^2 + (y \pm k)^2 = r^2 \quad (5)$$

where

$$k = d \sin \alpha$$

The simultaneous solution of equations (3) and (5) and substitution of $d \sin \alpha$ for k gives the intersection of these curves as

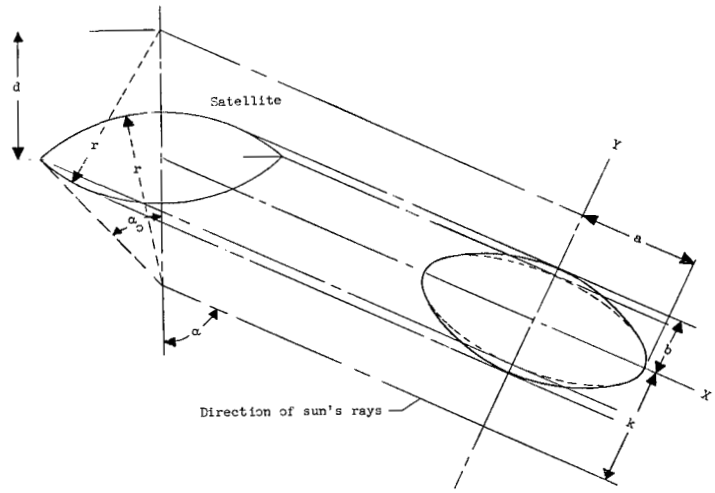

Figure 3.- Geometry of effective area of lenticular satellite.

$$y = \frac{\pm d \cos^2 \alpha}{\sin \alpha}$$

$$x = \pm\sqrt{r^2 - \frac{d^2}{\sin^2 \alpha}}$$

By using these points and the coordinate axes as integration limits, the following expression for A is readily obtained by elementary integration methods:

$$A = 2r^2 \left[\sin^2 \alpha_o \cos \alpha \left(\frac{\pi}{2} - \sin^{-1} \frac{X}{\sin \alpha_o \sin \alpha} \right) - X \cos \alpha_o + \sin^{-1} \frac{X}{\sin \alpha} \right] \quad (6)$$

in which

$$X = \sqrt{\sin^2 \alpha - \cos^2 \alpha_o}$$

Thus, equations (4) and (6) give the variation in A for all orientations of the satellite since the sun angle is in effect constrained to the interval $0 \leqq \alpha \leqq \frac{\pi}{2}$. The desired expression for the variation in $\overline{F}$ can now be obtained by substituting these results into equation (1).

The Perturbation Equations

The set of orbital elements and the differential equations for their rates of change given in reference 6 were used to calculate the perturbations due to solar radiation pressure. These equations may be expressed in the form:

$$\left.\begin{aligned}
\frac{da}{dt} &= \frac{2a^{3/2}F}{\sqrt{\mu}(1 - e\cos E)}\left(\hat{U}\cdot\hat{P}\sin E - \hat{U}\cdot\hat{Q}\sqrt{1 - e^2}\cos E\right)\\
\frac{de}{dt} &= \frac{\sqrt{a(1 - e^2)}F}{\sqrt{\mu}(1 - e\cos E)}\left[\hat{U}\cdot\hat{P}\sqrt{1 - e^2}\sin E\cos E\right.\\
&\quad \left. - \hat{U}\cdot\hat{Q}\left(\frac{3}{2} - 2e\cos E + \frac{1}{2}\cos 2E\right)\right]\\
\frac{di}{dt} &= \frac{a^{1/2}F\left(\hat{U}\cdot\hat{R}\right)}{\sqrt{\mu\left(1 - e^2\right)}}\left[\sqrt{1 - e^2}\sin E\sin\omega - (\cos E - e)\cos\omega\right]\\
\sin i\,\frac{d\Omega}{dt} &= \frac{-a^{1/2}F\left(\hat{U}\cdot\hat{R}\right)}{\sqrt{\mu\left(1 - e^2\right)}}\left[\sqrt{1 - e^2}\sin E\cos\omega + (\cos E - e)\sin\omega\right]\\
\frac{d\omega}{dt} + \cos i\,\frac{d\Omega}{dt} &= \frac{F}{e\sqrt{\mu}(1 - e\cos E)}\left[\hat{U}\cdot\hat{P}\sqrt{a\left(1 - e^2\right)}\left(\sin^2 E - e\cos E + 1\right)\right.\\
&\quad \left. - \hat{U}\cdot\hat{Q}\sqrt{a}\sin E(\cos E - e)\right]
\end{aligned}\right\} \qquad (7)$$

The quantities in these equations are defined in the list of symbols, and those having a geometrical interpretation are also defined in figure 4. An inertial equatorial coordinate system with the origin at the earth's center is used as the prime reference for the satellite motion and for the position of the sun which specifies the direction of $\overline{F}$ relative to the satellite orbit. In this system the X-axis is toward the vernal equinox, the Z-axis is along the earth's spin axis, and the Y-axis is taken to form an orthogonal system. The orientation of the orbit relative to the X, Y, Z axes is given by the angles i, ω, and Ω, and the position of the sun by ϵ and λ as shown in figure 4. Equations (7) also embody the frequently advantageous device of resolving the disturbing acceleration into components parallel and normal to the orbit plane. The unit vectors $\hat{P}$, $\hat{Q}$, and $\hat{R}$ are used for this purpose. Reference to figure 4 shows that $\hat{P}$ is directed along the semi-major axis toward the perigee point, $\hat{R}$ is normal to the orbit plane, and $\hat{Q}$ forms a

right-handed system. The scalar products appearing in equations (7) are given by the following relationships obtained from figure 4 by means of trigonometry

$$\left.\begin{aligned}
\hat{P} &= \hat{i}(\cos\omega\cos\Omega - \cos i\sin\omega\sin\Omega) \\
&\quad + \hat{j}(\cos\omega\sin\Omega + \cos i\sin\omega\cos\Omega) \\
&\quad + \hat{k}(\sin i\sin\omega) \\
\hat{Q} &= -\hat{i}(\sin\omega\cos\Omega + \cos i\cos\omega\sin\Omega) \\
&\quad - \hat{j}(\sin\omega\sin\Omega - \cos i\cos\omega\cos\Omega) \\
&\quad + \hat{k}(\sin i\cos\omega) \\
\hat{R} &= \hat{i}(\sin i\sin\Omega) - \hat{j}(\sin i\cos\Omega) + \hat{k}(\cos i) \\
\hat{U} &= \hat{i}(\cos\lambda) + \hat{j}(\cos\epsilon\sin\lambda) + \hat{k}(\sin\epsilon\sin\lambda)
\end{aligned}\right\} \qquad (8)$$

where $\hat{i}$, $\hat{j}$, and $\hat{k}$ are unit vectors along the X, Y, and Z axes.

Method of Calculating the Solar Pressure Perturbations

The method of Kryloff-Bogoliuboff is employed in reference 6 to obtain solutions to equations (7). When this method is applied, the integration is more conveniently accomplished by changing the independent variable from time to eccentric anomaly. This transformation is given by the relation

$$n\,dt = \frac{r}{a}\,dE$$

which is obtained from the theory of unperturbed conic motion. The solution of equations (7) is then accomplished on the digital computer by means of a fourth-order Runge-Kutta procedure in which the integration step corresponds to a time interval of

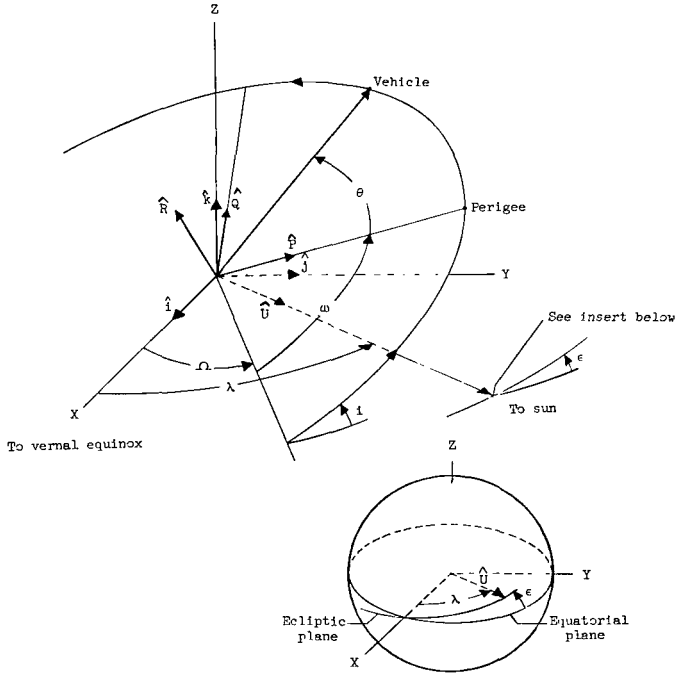

Figure 4.- Coordinate system.

1 day. The effect of shadowing of the satellite by the earth is accounted for by using the values of the eccentric anomaly at the points of exit and entry into the shadow region as integration limits.

This method is not as easily applied in the case of lenticular satellites because of the variation in $\bar{F}$. Instead of determining an average value of $\bar{F}$ over the illuminated portion of the orbit and then applying the method described, a somewhat different approach was used. This procedure involves calculating $\bar{F}$ by means of equations (4) and (6) for each degree of mean anomaly, using the results in equations (7) to obtain the corresponding rates of change of the orbital elements, and then finding the average rates of change over one full orbital revolution. The effect of shadowing is taken into account by subtracting out the shadow region in the averaging process.

THE NATURE OF SOLAR PRESSURE PERTURBATIONS

To facilitate discussion of the results, the processes by which solar-radiation pressure alters the elements of a satellite orbit are briefly described. It is convenient for this purpose to divide the orbital elements into two groups. The elements a and e which specify the orbit size and shape form one group, and its orientation elements i, ω, and Ω comprise the other. The sixth element is time which specifies the satellite position in its orbit and serves as the independent variable. In addition, the conditions for which resonances can occur are also included.

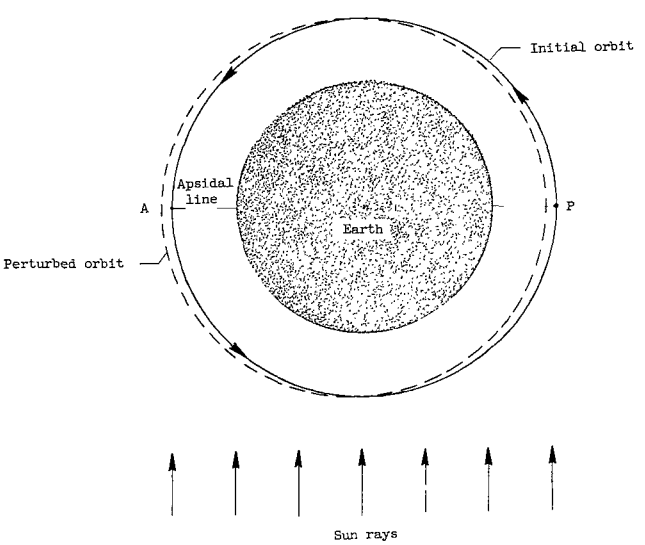

Figure 5.- Illustration of change in eccentricity.

The Changes in Orbit Size and Shape

The change in eccentricity.- The process by which solar radiation pressure changes the eccentricity e can be described with the aid of figure 5 which represents an initially circular orbit oriented parallel to the sun's rays. As the satellite moves away from the sun in the region of point P, solar pressure accelerates its motion and thereby causes it to recede to a higher altitude. The situation is reversed in the vicinity of point A where solar pressure decelerates the motion, and causes the satellite then to seek a lower altitude. Evidently, the continuation of this process causes e to increase, and will create a perigee

at P and an apogee at A provided the sun direction does not change relative to the apsidal line PA that is produced normal to the sun line. Thus, the increasing apogee and decreasing perigee heights that accompany the change in e results in translation of the orbit along the line PA toward A. If the sun position relative to PA of the perturbed orbit illustrated in figure 5 were to be changed by 180°, e would decrease to zero and then increase in the manner just described, except that the perigee would be created at point A.

A third type of behavior in which the net change in e per orbital revolution is zero arises when the apsidal line of an elliptical orbit is oriented parallel to the sun direction. This result can be inferred from the expression for de/dt in equations (7) since $\hat{U} \cdot \hat{Q}$ is zero for this situation. Thus, the change in e depends on the orientation of the apsidal line relative to the direction of the solar disturbing force. Since the apsidal line moves with respect to the sun line, except when resonant conditions are present, e must generally vary in a periodic manner. The period of this oscillation is evidently equal to the time required for the apsidal line to rotate once relative to the sun position.

The effect of shadow.- The portion of the potential energy of a satellite that is associated with the solar-radiation pressure field is a function of its distance from the sun. (See eq. (2).) When the satellite is continuously illuminated by the sun, the solar pressure force is conservative and no change in energy occurs over a complete orbital revolution. For orbit orientations where the satellite passes through the region of the shadow cast by the earth, the solar pressure force is not conservative and a net change in energy can take place. The situations for which energy changes can occur are illustrated in figure 6.

If the shadow region is located at position A as shown in figure 6, the satellite will emerge from shadow at a point further from the sun than the point where it entered. Since the solar pressure force is zero in the shadow region, the satellite gives up an amount of potential energy proportional to the difference in the distances of the two points from the sun. The opposite behavior occurs if the shadow occurs at position B where the satellite then gains potential energy. No change in energy occurs for positions C or D since the entry and exit points of the shadow region are of equal distance from the sun. Thus, the energy change due to shadowing depends on the orientation of the shadow region relative to the apsidal line. Since the shadow location depends on the position of the apsidal line CD with respect to the sun, it is evident that the change in energy due to shadow varies in a manner similar to the eccentricity and with the same period.

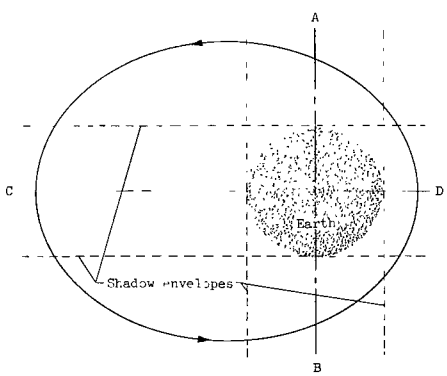

Figure 6.- Sketch used in describing change in energy due to shadowing.

The Change in Orbit Orientation

The effects of solar radiation pressure on the orbit orientation elements i, ω, and Ω are small in most instances. For given values of a and F, equations (7) show that the rates of change of these elements depend mainly on the eccentricity. As e increases, the combined effect of $\sqrt{\mu a(1 - e^2)}$ and the long-period terms $e \cos \omega$ and $e \sin \omega$ can produce noticeable changes in the elements i and Ω. The presence of $\sin i$ in the denominator of the expression for $d\Omega/dt$ can lead to large changes in Ω for small values of i. However, the third harmonic of the earth's gravitational potential dominates the change in Ω as i becomes small for the area-mass ratios considered in this study.

In contrast, the occurrence of e as a divisor in the expression for $d\omega/dt$ can cause ω to change rapidly whenever e becomes small. Since the rate at which the apsidal line moves depends on $d\omega/dt$ and $d\Omega/dt$, it is clear that ω can have an important effect on the period of a and e. The presence of resonances, which are described in the next section, can cause significant changes in i, ω, and Ω. When resonant conditions exist, the scalar products of $\hat{P}$, $\hat{Q}$, and $\hat{R}$ with $\hat{U}$ contain secular terms.

Resonances

The situation depicted in figure 5 represents a resonant condition that can eventually destroy the orbit. Resonances occur whenever the apsidal line maintains, on the average, a constant orientation relative to the disturbing force. It is shown in reference 11 that there are six conditions for which equations (7) become resonant. By starting with equations (8) and using trigonometric identities, the quantities in equations (7) that involve scalar products of $\hat{P}$, $\hat{Q}$, and $\hat{R}$ with $\hat{U}$ may be written

$$\left.\begin{aligned} \hat{U} \cdot \hat{P} = {} & \cos^2 \frac{i}{2}\left[\cos^2 \frac{\epsilon}{2} \cos(\omega + \Omega - \lambda) + \sin^2 \frac{\epsilon}{2} \cos(\omega + \Omega + \lambda)\right] \\ & + \sin^2 \frac{i}{2}\left[\cos^2 \frac{\epsilon}{2} \cos(\omega - \Omega + \lambda) + \sin^2 \frac{\epsilon}{2} \cos(\omega - \Omega - \lambda)\right] \\ & + \frac{1}{2} \sin i \sin \epsilon \left[\cos(\omega - \lambda) - \cos(\omega + \lambda)\right] \end{aligned}\right\} \qquad (9)$$

Equations (9) are continued on next page

$$
\left.
\begin{aligned}
\hat{U} \cdot \hat{Q} &= -\cos^2 \tfrac{i}{2}\left[\cos^2 \tfrac{\epsilon}{2} \sin(\omega + \Omega - \lambda) + \sin^2 \tfrac{\epsilon}{2} \sin(\omega + \Omega + \lambda)\right] \\
&\quad - \sin^2 \tfrac{i}{2}\left[\cos^2 \tfrac{\epsilon}{2} \sin(\omega - \Omega + \lambda) + \sin^2 \tfrac{\epsilon}{2} \sin(\omega - \Omega - \lambda)\right] \\
&\quad - \tfrac{1}{2} \sin i \sin \epsilon\left[\sin(\omega - \lambda) - \sin(\omega + \lambda)\right] \\
\hat{U} \cdot \hat{R} \sin \omega &= \tfrac{1}{2} \sin i\left\{\cos^2 \tfrac{\epsilon}{2}\left[\cos(\omega - \Omega + \lambda) - \cos(\omega + \Omega - \lambda)\right]\right. \\
&\quad \left. + \sin^2 \tfrac{\epsilon}{2}\left[\cos(\omega - \Omega - \lambda) - \cos(\omega + \Omega + \lambda)\right]\right\} \\
&\quad + \tfrac{1}{2} \cos i \sin \epsilon\left[\cos(\omega - \lambda) - \cos(\omega + \lambda)\right] \\
\hat{U} \cdot \hat{R} \cos \omega &= \tfrac{1}{2} \sin i\left\{\cos^2 \tfrac{\epsilon}{2}\left[\sin(\omega + \Omega - \lambda) - \sin(\omega - \Omega + \lambda)\right]\right. \\
&\quad \left. + \sin^2 \tfrac{\epsilon}{2}\left[\sin(\omega + \Omega + \lambda) - \sin(\omega - \Omega - \lambda)\right]\right\} \\
&\quad + \tfrac{1}{2} \cos i \sin \epsilon\left[\sin(\omega + \lambda) - \sin(\omega - \lambda)\right]
\end{aligned}
\right\} \qquad (9)
$$

Hence each expression in equations (7) contains sines or cosines of all six of the arguments

$$
\left.
\begin{aligned}
\omega \pm \Omega \pm \lambda &= (\dot{\omega} \pm \dot{\Omega} \pm \dot{\lambda})t + \left(\omega_o \pm \Omega_o \pm \lambda_o\right) \\
\omega \pm \lambda &= (\dot{\omega} \pm \dot{\lambda})t + \left(\omega_o \pm \lambda_o\right)
\end{aligned}
\right\} \qquad (10)
$$

If any one of the following conditions is fulfilled

$$
\left.
\begin{aligned}
\text{I.} \quad & \dot{\omega} + \dot{\Omega} + \dot{\lambda} = 0 \\
\text{II.} \quad & \dot{\omega} - \dot{\Omega} - \dot{\lambda} = 0 \\
\text{III.} \quad & \dot{\omega} + \dot{\Omega} - \dot{\lambda} = 0
\end{aligned}
\right\} \qquad (11)
$$

Equations (11) are continued on next page

$$\left.\begin{aligned} &\text{IV.} \quad \dot{\omega} - \dot{\Omega} + \dot{\lambda} = 0 \\ &\text{V.} \quad \dot{\omega} + \dot{\lambda} = 0 \\ &\text{VI.} \quad \dot{\omega} - \dot{\lambda} = 0 \end{aligned}\right\} \tag{11}$$

its corresponding argument in equations (10) will remain constant. In all such cases, each expression in equations (9) will contain a secular term involving either the sine or cosine of the argument the rate of change of which vanishes in accordance with equations (11). Furthermore, it is clear that the resulting resonant behavior will progress at the maximum rate when the initial values of ω, Ω, and λ result in sine or cosine terms that are unity. As indicated in the section describing the change in eccentricity, it is precisely this situation for which the change in e due to solar radiation pressure is greatest. It is to be emphasized that it is not the conditions for resonance given by equations (11), but the ensuing resonant changes in the orbital elements that are caused by solar radiation pressure.

If the method of reference 11 is followed, equations (11) may be used to calculate the resonant inclinations for any combination of a and e. The first-order approximation used in this method appears to be adequate for most purposes. To first order, the time rates of ω and Ω are dominated by the second harmonic of the earth's gravitational potential and are given by

$$\left.\begin{aligned} \dot{\omega} &= \frac{1}{2} \frac{nA_2}{a^2\left(1 - e^2\right)^2}\left(5 \cos^2 i - 1\right) \\ \dot{\Omega} &= - \frac{nA_2}{a^2\left(1 - e^2\right)^2} \cos i \end{aligned}\right\} \tag{12}$$

The substitution of these expressions into equations (11) yields a set of quadratic equations in $\cos i$ the roots of which give the resonant inclinations.

RESULTS AND DISCUSSION

The computational procedure contained in this report was used to obtain time histories of the satellite's orbital elements for a period of 1 year. Numerical data were generated for seven orbital inclinations ranging from 0° to 113° to determine the effect of the sun position relative to the orbit plane and to examine resonances. All the calculations were made with an initial eccentricity of 0.001 and an initial altitude of 2,000 nautical miles which is considered a desirable altitude for passive communications satellites.

The results of the study are presented in terms of e and ω since the perturbations in the elements a, i, and Ω were found to have only a small effect on e for the seven cases that were examined. Data for the argument of

perigee are included because of the influence of ω on the period of the oscillation in e as described in the section on perturbations. Resonances are discussed in terms of table I which contains the rates of the six arguments given by equations (10) for each of the seven orbital inclinations. The entries in table I serve to indicate the resonant tendencies in each case. Finally, results from two of the lenticular runs are compared on an equal area-mass ratio basis with corresponding data for a sphere.

TABLE I.- RESONANT TENDENCIES OF LONG-PERIOD ARGUMENTS

[Underlined values indicate resonant condition most closely approached]

Resonant condition	Rate of change of long-period argument	Values of rates of change of long-period argument in radians per day for -						
		Case A: $i = 0.5^\circ$	Case B: $i = \epsilon$	Case C: $i = \epsilon + 10^\circ$	Case D: $i = \epsilon + 30^\circ$	Case E: $i = 70^\circ$	Case F: $i = \epsilon + 60^\circ$	Case G: $i = \epsilon + 90^\circ$
I	$\dot{\omega} + \dot{\Omega} + \dot{\lambda}$	0.0422	0.0412	0.0314	0.0099	-0.0032	<u>-0.0020</u>	0.0275
II	$\dot{\omega} - \dot{\Omega} - \dot{\lambda}$	.0878	.0711	.0554	.0172	-.0296	-.0125	-.0350
III	$\dot{\omega} + \dot{\Omega} - \dot{\lambda}$	<u>.0078</u>	<u>.0068</u>	<u>-.0030</u>	-.0245	-.0376	-.0364	-.0069
IV	$\dot{\omega} - \dot{\Omega} + \dot{\lambda}$	.1222	.1055	.0898	.0516	.0048	.0219	<u>-.0004</u>
V	$\dot{\omega} + \dot{\lambda}$	.0872	.0734	.0506	.0307	<u>.0008</u>	.0099	.0209
VI	$\dot{\omega} - \dot{\lambda}$	.0528	.0390	.0262	<u>-.0037</u>	-.0336	-.0245	.0136

The Changes in Eccentricity and Argument of Perigee

The time histories of e are plotted in figure 7 for each of the seven orbital inclinations. All these curves exhibit the same type of large-amplitude, long-period variation that is obtained for spherical configurations. These results indicate that the minimum amplitude of e occurs for an inclination in the vicinity of 70°. However, even in this case e is large enough to affect the stability of the satellite's attitude motion. (See ref. 4.)

Figure 8 contains the corresponding plots of the variation of ω with t. Comparisons of these curves with those of figure 7 indicate that ω varies in a uniform manner when e is not near zero. However, the last of equations (7) predicts that, if the eccentricity is small, large net variations in ω per orbital revolution can occur unless the sun is normal to the apsidal line. The results for $i = 70^\circ$ confirm this prediction. Figure 7 shows that e decreases to approximately 0.017 in the region of the 167-day point on the plot. Accordingly, the slope of ω is large at the corresponding point on figure 8. In the vicinity of 274 days, e reaches a lower minimum of about 0.001, and the slope of ω becomes nearly vertical. A similar large change in ω does not occur at the starting point because the initial conditions were chosen such that the sun was normal to the apsidal line. To obtain physically correct

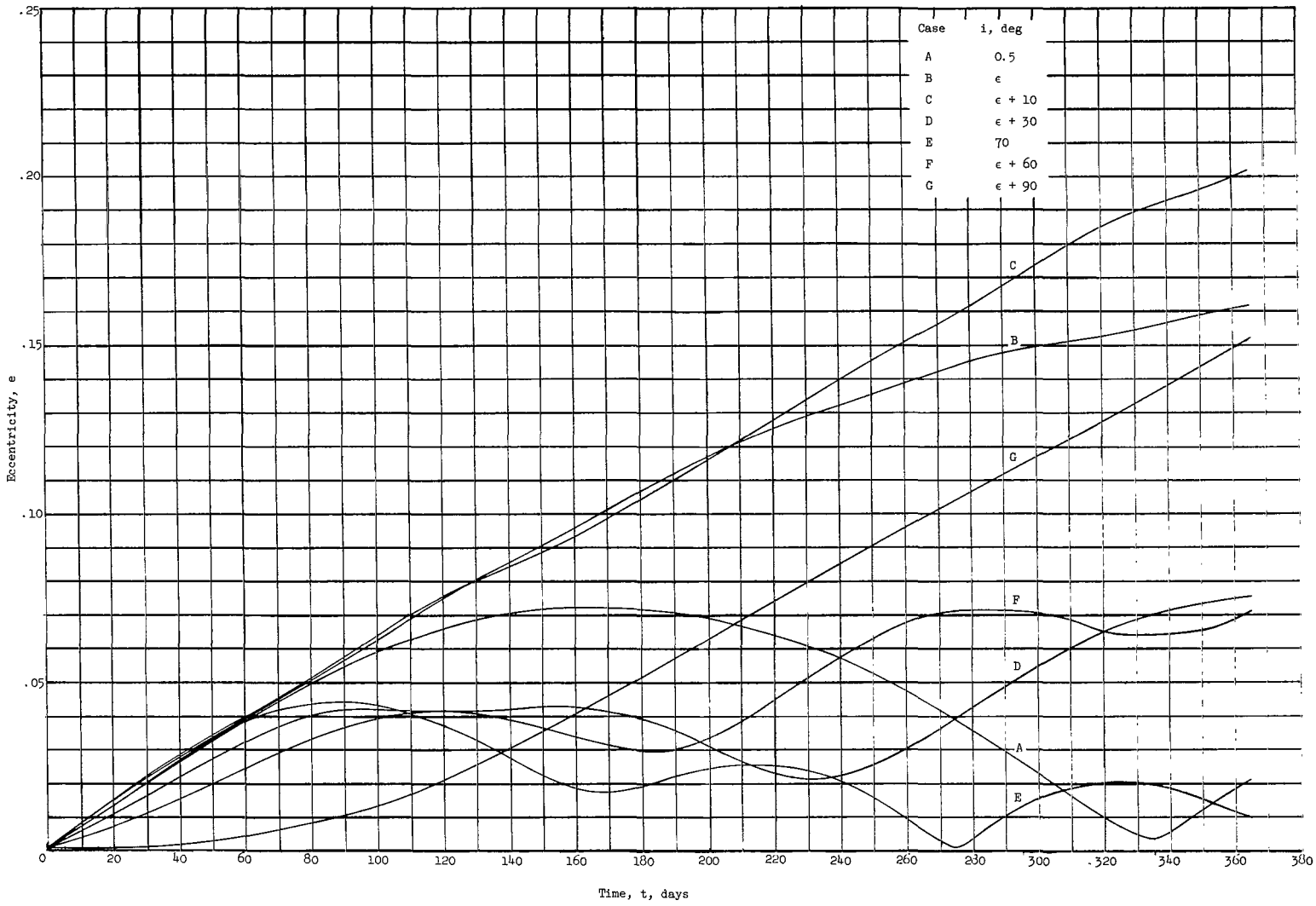

Figure 7.- Time histories of eccentricity.

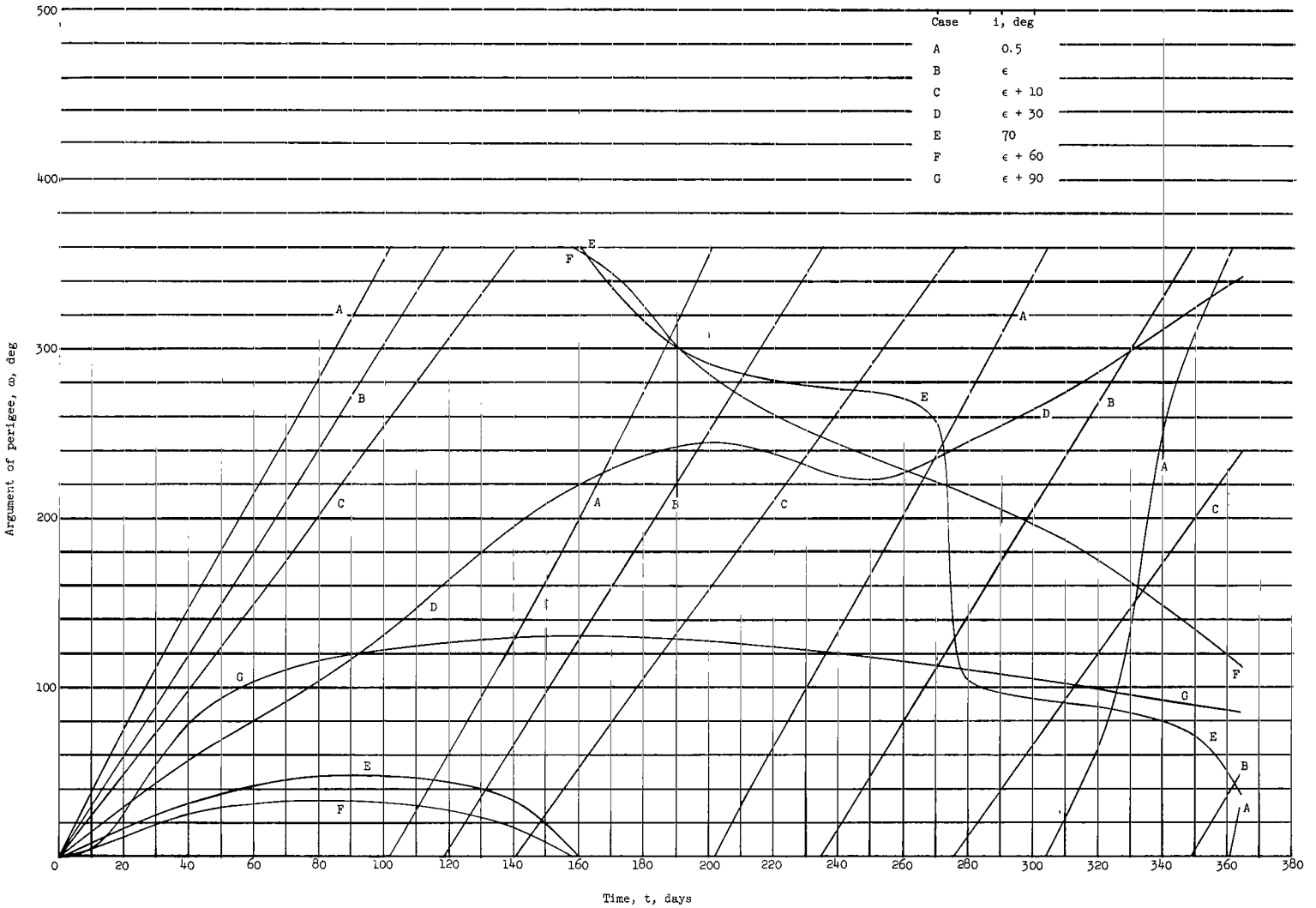

Figure 8.- Time histories of argument of perigee.

results, it is important to choose initial conditions so that e does not decrease to zero before increasing since the resulting small divisor would invalidate equations (7).

Resonances

The resonant tendencies of a given orbit can be easily identified by tabulating the left-hand members of equations (11) as was done in reference 12. This information was computed for the seven cases and is presented in table I. The entries in this table are expressed in radians per day. For each inclination, the resonant condition most closely approached is indicated by the smallest entry which is underlined in the table.

Although the tabular arrangement is useful, the tendencies toward resonance can be more clearly illustrated by plotting the rates of change of equations (10) as functions of orbital inclination. Figure 9 presents this information for the initial values of altitude and eccentricity used in the study. The resonant inclinations for all six conditions are easily located since the points where each curve passes through zero are obviously the roots of equations (11). Thus these curves not only indicate the resonant tendencies for a given orbit inclination, but also provide a means of identifying which of the six resonant conditions is most closely approached.

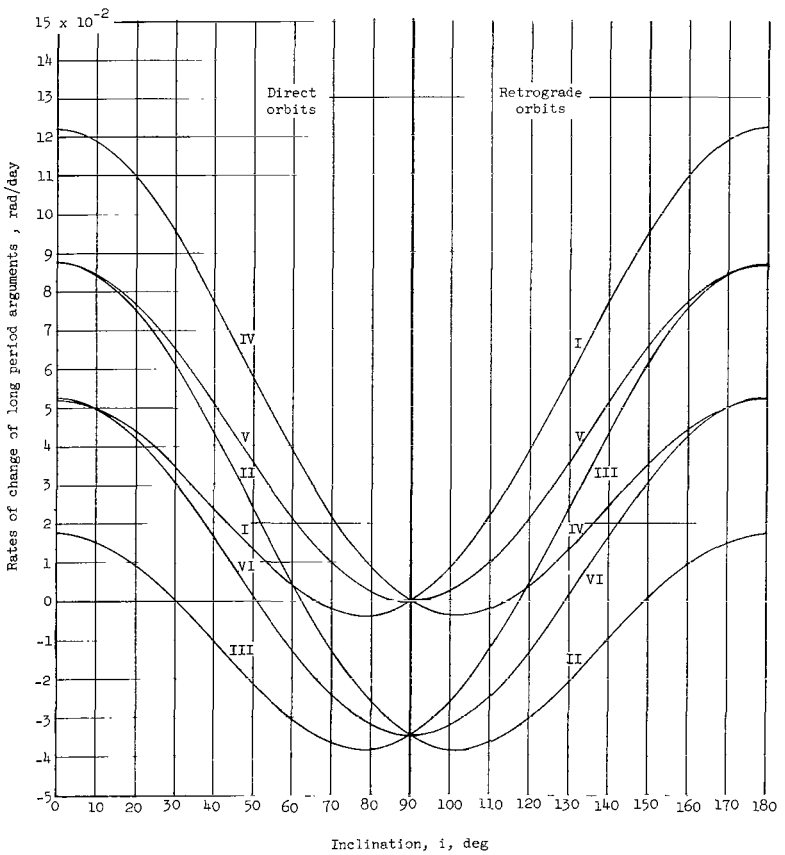

Figure 9.- Variation of resonant conditions with orbital inclination. Roman numerals indicate resonant conditions.

As mentioned earlier, two of the seven orbital inclinations were chosen to yield resonances. The two cases selected for this purpose are cases C and G. Reference to table I and figure 9 shows that case C approaches the resonance given by condition III of equations (11). The proximity to condition III is reflected by the large-amplitude long-period variation in curve C of figure 7. Similar results are obtained for case G where the behavior of curve G is dominated by resonant condition IV.

Cases D, E, and F were not intended to correspond

to resonant conditions; however, inspection of table I shows that all three are nearly resonant. Table I also indicates that each of these three cases is near more than one resonant condition at the same time. This situation illustrates how the dominant resonant condition changes from one to another as the orbital inclination is varied. Figure 9 indicates that these changes can occur for relatively small increments in i when the orbital inclination is between 60° and 120°. The curves in figure 9 not only illustrate why "bundles of resonances" occur for nearly polar orbits, but also indicate which of the six resonant conditions causes each such bundle.

Comparison of Lenticular and Spherical Configurations

For perfectly absorptive bodies, the difference in the force exerted by solar radiation pressure on a lenticule and on a sphere is due to the variation in the effective area of the lenticule. A comparison of the orbital eccentricities for the two configurations is presented in figure 10 for cases B and E, respectively. Using an area-mass ratio equal to the maximum value for the lenticule, data for cases B and E were calculated for the spherical configuration. Comparisons of the two configurations indicate that the oscillations in e have nearly the same periods and differ mainly in their amplitudes for both cases B and E. On the basis of these results, cases B and E were rerun for the spherical configuration using area-mass ratios equal to the average values for the lenticular configuration over a 1-year period. These data are presented in figure 10. Figure 10 shows that the time histories of e agree fairly well when the two configurations are compared on an equal area-mass ratio basis.

Although this approximation yields good agreement, it assumes a constant value for the average area-mass ratio which ignores a long-period variation that arises because of the change in the orbit orientation relative to the sun direction. For this reason, the average area-mass ratio for a given day in the year will differ from that for some other day so that an average area-mass ratio based on a period of a year will not represent the true value over some portions of the 1-year period with sufficient accuracy. Therefore, if the average area-mass ratio is determined at more frequent intervals to account for this long-period variation, the curves in figure 10 should agree more closely. Another source of discrepancy not accounted for in the averaging process is the fact that the energy change due to shadowing is also affected by the long-period variation just mentioned. However, this effect can be ignored since its influence on e is small. Thus, the principal part of the variation in the effective area-mass ratio of a lenticular satellite appears to behave much like a short-period term in the disturbing function.

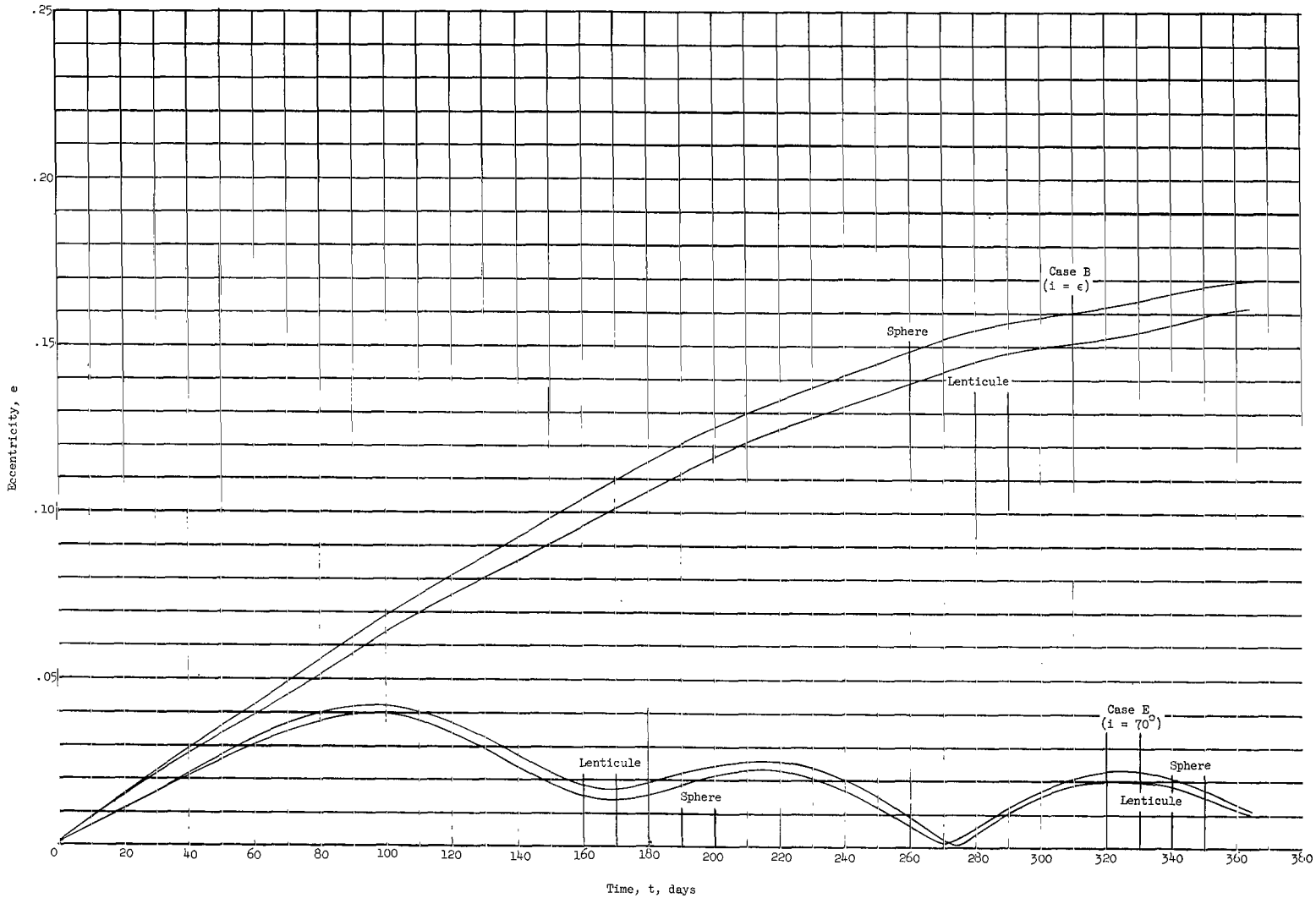

Figure 10.- Comparison of eccentricities for a lenticular and a spherical satellite.

CONCLUDING REMARKS

A study of the orbital motion of a gravity-gradient-oriented lenticular satellite has indicated that solar-radiation pressure alters the orbital eccentricities of lenticular and spherical configurations in much the same manner. The following remarks are stated on the basis of the results obtained:

1. The perturbations due to solar radiation pressure are sufficiently severe that a means of controlling the eccentricity appears necessary for lenticular satellites unless the problem can be substantially avoided through the use of mesh materials or some other alternative.

2. The principal variation in the effective area-mass ratio of a lenticular satellite is due to the short-term oscillation in its orientation relative to the sun's rays and appears to behave much like a short-period term in the disturbing function which tends to average out.

3. Good agreement with results for a sphere, using an area-mass ratio equal to the average value for the lenticular configuration, is obtained provided the time period over which the area-mass ratio is averaged is small enough to neglect long-period variations in the effective area of the satellite.

Langley Research Center,
National Aeronautics and Space Administration,
Langley Station, Hampton, Va., December 3, 1964.

REFERENCES

1. Reiger, S. H.: A Study of Passive Communications Satellites. R-415-NASA (NASr-20(02)), The RAND Corp., Feb. 1963.

2. Fischell, Robert E.; and Mobley, Frederick F.: A System for Passive Gravity-Gradient Stabilization of Earth Satellites. TG 514, Appl. Phys. Lab., The Johns Hopkins Univ., Aug. 1963. (Also available as AIAA Paper No. 63-326.)

3. Baker, Robert M. L., Jr.: Librations on a Slightly Eccentric Orbit. ARS J., vol. 30, no. 1, Jan. 1960, pp. 124-126.

4. DeBra, D. B.: Attitude Stability and Motions of Passive, Gravity-Oriented Satellites. Vol. 11 of Advances in Astronautical Sciences, Horace Jacobs, ed., Western Periodicals Co. (N. Hollywood, Calif.), c.1963, pp. 99-118.

5. Musen, Peter: The Influence of the Solar Radiation Pressure on the Motion of an Artificial Satellite. J. Geophy. Res., vol. 65, no. 5, May 1960, pp. 1391-1396.

6. Bryant, Robert W.: The Effect of Solar Radiation Pressure on the Motion of an Artificial Satellite. NASA TN D-1063, 1961.

7. Bryant, R. W.: A Comparison of Theory and Observation of the Echo I Satellite. NASA TN D-1124, 1961.

8. Zadunaisky, Pedro E.; Shapiro, Irwin I.; and Jones, Harrison M.: Experimental and Theoretical Results on the Orbit of Echo I. Special Rept. No. 61, Smithsonian Institution Astrophysical Observatory, Mar. 20, 1961.

9. Shapiro, Irwin I.: Sunlight Pressure Perturbations on Satellite Orbits. Vol. 11 of Advances in Astronautical Sciences, Horace Jacobs, ed., Western Periodicals Co. (N. Hollywood, Calif.), c.1963, pp. 35-60.

10. Kozai, Yoshihide: Effects of Solar Radiation Pressure on the Motion of an Artificial Satellite. Special Rept. No. 56, Smithsonian Institution Astrophysical Observatory, Jan. 30, 1961.

11. Wyatt, Stanley P.: The Effect of Radiation Pressure on the Secular Acceleration of Satellites. Special Rept. No. 60, Smithsonian Institution Astrophysical Observatory, Mar. 10, 1961.

12. Polyakhova, Ye. N.: Solar Radiation Pressure and the Motion of Earth Satellites. AIAA J. (Russian Suppl.), vol. 1, no. 12, Dec. 1963, pp. 2893-2909.

2/22/85

"The aeronautical and space activities of the United States shall be conducted so as to contribute . . . to the expansion of human knowledge of phenomena in the atmosphere and space. The Administration shall provide for the widest practicable and appropriate dissemination of information concerning its activities and the results thereof."

—NATIONAL AERONAUTICS AND SPACE ACT OF 1958

NASA SCIENTIFIC AND TECHNICAL PUBLICATIONS

TECHNICAL REPORTS: Scientific and technical information considered important, complete, and a lasting contribution to existing knowledge.

TECHNICAL NOTES: Information less broad in scope but nevertheless of importance as a contribution to existing knowledge.

TECHNICAL MEMORANDUMS: Information receiving limited distribution because of preliminary data, security classification, or other reasons.

CONTRACTOR REPORTS: Technical information generated in connection with a NASA contract or grant and released under NASA auspices.

TECHNICAL TRANSLATIONS: Information published in a foreign language considered to merit NASA distribution in English.

TECHNICAL REPRINTS: Information derived from NASA activities and initially published in the form of journal articles.

SPECIAL PUBLICATIONS: Information derived from or of value to NASA activities but not necessarily reporting the results of individual NASA-programmed scientific efforts. Publications include conference proceedings, monographs, data compilations, handbooks, sourcebooks, and special bibliographies.

Details on the availability of these publications may be obtained from:

SCIENTIFIC AND TECHNICAL INFORMATION DIVISION

NATIONAL AERONAUTICS AND SPACE ADMINISTRATION

Washington, D.C. 20546